ULTRAWIDEBAND MODELING OF TRANSMIT AND RECEIVE ANTENNA SYSTEMS

Tapan K. Sarkar
Department of Electrical Engineering and Computer Science
323 Link Hall, Syracuse University
Syracuse, New York 13244-1240
tksarkar@syr.edu, http://web.syr.edu/ ~tksarkar

Abstract

Broadband characterisations are very useful in many applications as they operate over a wide range of frequencies. The objective of this paper is to study the transient responses of various well-known antennas over broad frequency ranges. As such, the phase responses of these antennas as a function of frequency are of great interest. Broadband characterization without the phase response is an incomplete analysis of the problem. In the ensuing analysis, each antenna is excited by a monocycle pulse. Many antennas show resonant properties, and numerous reflections exist in the antenna outputs However, some of the antennas are inherently broadband, up to a 100:1 bandwidth. Hence, the transient responses of these antennas can be used to determine their suitability for wideband applications with low cutoff frequency. This paper illustrates the radiation and reception properties of various conventional ultrawideband (UWB) antennas in the time domain. Examples are presented to illustrate the various systems

1. INTRODUCTION

One area that has drawn a lot of attention is the channel modeling of free space for a broadband wireless system. This sounds very surprising at the first look because in the Maxwell's theory air is typically assumed to be dispersionless, and so, why model a dispersionless channel? However, many researchers are used to only looking at the channel and not consider the effect of the transmitting and the receiving antennas which are an integral part of a wireless system. Now, if one looks at Frii's transmission formula one observes that any transmitted signal strength will decay as $1/\lambda^2$ in free space due to the propagation of the spherical wave from a source. If such were the case, it will really be a highly dispersive channel. However, particularly for a broadband wireless system, one cannot only think about the isolated channel without the associated transmitting and receiving antennas, as they form an integral part of a wireless system. With the transmitting and the receiving antennas included in the broadband model, things behave in quite a different way. The gain of any transmitting antenna increases with $1/\lambda$ and so does the gain of any receiving antenna, which increases also with $1/\lambda$. Therefore, with the transmitting and the receiving antennas in a broadband wireless transmission system, Frii's transmission loss is compensated for by the two antennas making the channel completely dispersionless over a large band. We will illustrate it by measured experimental data obtained by James R. Andrews of the Picosecond Pulse Lab [1]. A step function with an amplitude of 4 V and of rise time 9 ps was applied to the apex of a transmitting bicone antenna. This ultra-broadband test input signal used was from an experimental NLTL pulser, Fig. 1. When using a conical transmitting antenna, the incident E field, onto the receive TEM horn antenna is a close replica of this waveform. All of the waveforms shown in this paper were measured using a HP-54752B, 50 GHz, 9 ps risetime, oscilloscope. A 35 cm, Gore, SMA coaxial cable was used to connect the antennas to the oscilloscope. The risetime of this cable was 9 ps. Thus the composite risetime of the pulse generator, coax cable and oscilloscope was an additional 16 ps. The bicone antenna is situated on top of a ground plane and was 7 cm high. The radiated fields are received by a 15 cm long TEM horn antenna, half of which is situated over a ground plane. The received waveform at the TEM horn when the separation distance between the bicone and the TEM horn is 25 cm is shown in Fig. 2 a). This will definitely be a near field scenario. By observing Figs. 1 and 2 a) it is seen that the received waveform is an excellent replica of the applied input step. Next, the TEM horn antenna is separated form the bicone by a distance of 5 m. This will be a typical far field scenario. In this case the measured waveform is shown in Fig. 2 b), which again is an excellent replica of the input waveshape demonstrating that this wireless transmission-reception system is dispersionless over a very large bandwidth!

The moral of the story is that the transmitting and the receiving antennas must be included in the modeling of a wireless channel to make the results meaningful for any system applications. And when special classes of transmitting and receiving antennas are considered, one can make the wireless channel completely dispersionless as shown by the experimental data [1] obtained by James R. Andrews. This setup produces a completely dispersionless system as a bicone antenna on transmit does not distort the initial waveshape, whereas a TEM horn on receive does not distort the received waveform either, thereby resulting in a distortionless transmission.

In summary, the important point to observe is that an acoustic signal is not distorted when it is converted to electrical energy through any microphone or when the electrical energy is converted to acoustic energy through any loudspeaker. However, the problem is quite different for the vector electromagnetic problem. In the time domain, the impulse response of the antenna when it is operating in the transmit mode is the time derivative of the impulse response when the same antenna is operating in the receive mode. Therefore, any broadband wireless system modelling ***must*** factor into the ***antenna effects*** to obtain a physically meaningful solution.

Next we describe some real ultra wideband antennas.

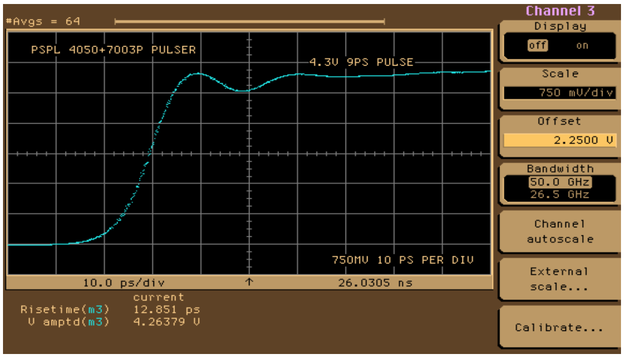

Figure 1. A 4 V 9 ps step applied to a 7 cm long bicone antenna.

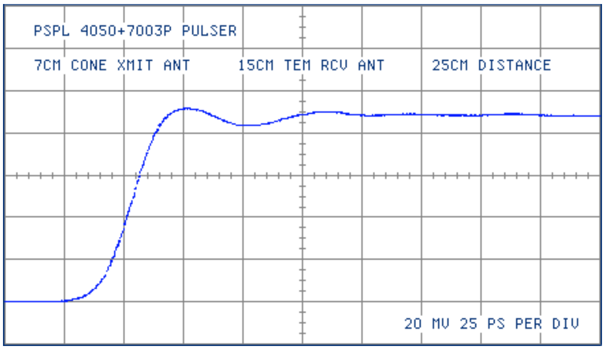

Figure 2 a): at a distance of 25 cm

2. ULTRAWIDEBAND ANTENNAS – CENTURY BANDWIDTH ANTENNAS

The bi-blade antenna is designed for multi-octave transmission with a century bandwidth. Due to its century bandwidth of operation, the bi-blade radiates and receives at UHF, L, C, S, and X bands [2]. Each of the two blades has a throat (narrowest part), a mouth (widest part), and a tip. The throat serves as the feed point. The tip is an arc of constant radius, thereby giving rise to a low voltage standing wave ratio of about 1.19 to 1 [2]. The radius of the arc determines the slope of the antenna's surge impedance. The blades are designed such that the slot width between the two blades increases logarithmically from the throat to the mouth of the antenna as shown in Fig. 3. The blade length is 0.56 m and the maximum slot width is 0.43 m. The blade is 0.11 m wide at its mouth. The antenna has a coplanar geometry and thus is easy to integrate into many systems. The antenna is fed by a generator placed between the two blades at the throat. The feed wire connecting the two blades of the antenna has a length of 4 mm and a radius of 0.01 mm. The origin of the coordinate system is the midpoint of the feed wire.

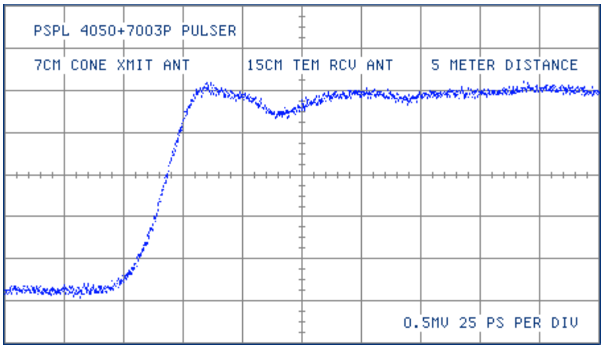

Figure 2 b): at a distance of 5 m

Figure 2: Plot of the received waveshape at a TEM receiving horn antenna situated at various distances from the transmitting monocone situated on top of a ground plane.

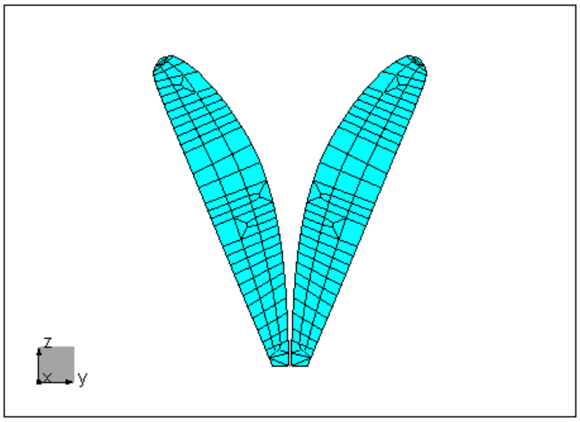

Figure 3. A bi-blade century bandwidth antenna.

The antenna is simulated between 160 MHz and 16 GHz, the time support of the response determined by the lowest frequency of operation is 1.875 lm, and the width of the input pulse is 0.075 lm. The antenna radiates along the *z*-axis of Fig. 3, and the polarization of the radiated field is along the *y*-axis on the *yz*-plane. The radiated field due to a monocycle pulse has a strong return and a weak reflected pulse corresponding to the reflection from the tip of the antenna (Fig. 4), which implies that the antenna does not have significant phase dispersion. The x-axis labelled *lm* represent the unit light meter. It is the time taken by light to propagate 1 m in free space. The use of this unit for time normalizes the various plots and uses fewer parameters to express the desired results. The first pulse is a good approximation of the input monocycle. When the antenna is illuminated by a monocycle pulse arriving along the z-axis, the induced current roughly has the same general shape as the incident field but with significant differences (Fig. 5). In particular, the current increases to a value that is commensurate with its maximum positive excursion. The transient input resistance of the antenna in response to a monocycle pulse is shown in Fig. 6.

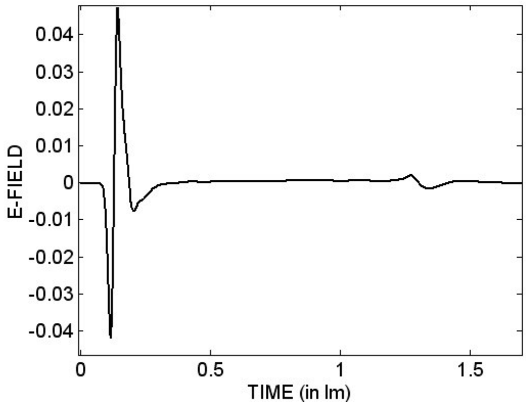

Figure 4. Radiation from a bi-blade antenna.

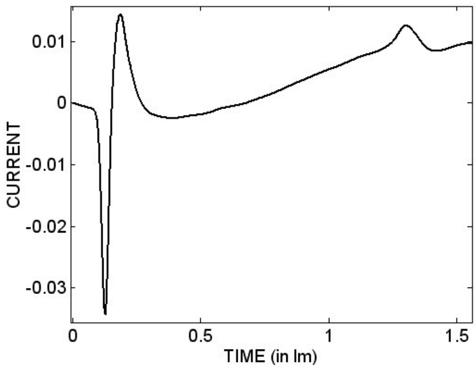

Figure 5. Reception of a monocycle by a bi-blade antenna.

3. CONE-BLADE ANTENNA

The cone-blade [3] is a circularly polarized antenna structure based on the conical antenna and is a modification of the bi-blade century bandwidth antenna. The cone-blade structure is a truncated closed half cone that is surrounded by four equally spaced blades that are separated by 90° (Fig. 7). The supporting base of the antenna is the flat truncated portion of the cone, and the blades are thin conducting plates that are placed near the base of the cone and extend upwards in the same direction as the cone's vertex. The cone has a half angle of 11.53° and a height of 0.228 m. The antenna is fed via a quadri-phase monocycle excitation by four generators, one at each of the four wires connecting the blade and the cone. Each generator has a 90° phase shift from the generator on the adjacent feed arm. Since the main beam of the radiation pattern at each frequency points along the cone's axis (z-axis), the simulated far field is calculated at an observation point along the positive z-axis. Each of the feed wires has a length of 20 mm and a radius of 0.01 mm. The antenna is simulated between 200 MHz to 20 GHz, and the width of the input pulse is 0.06 lm.

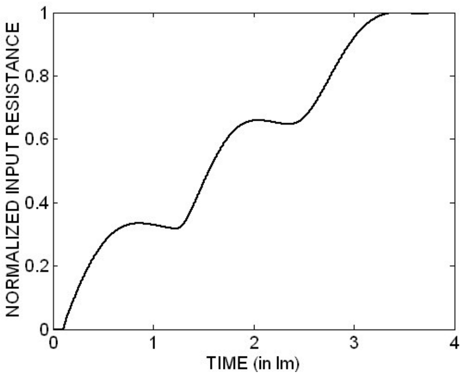

Figure 6. Transient input resistance of a bi-blade antenna.

The observed radiated field and the second derivative of the monocycle are shown in Fig. 8. Since no reflected pulses are present in the field and the curves almost coincide, this antenna is a traveling-wave antenna. For reception, the current induced in the antenna from a circularly polarized monocycle field that is incident along the z-axis is shown in Fig. 9. The induced current has no components associated with reflections along the antenna, thereby providing further verification that the antenna is a traveling-wave structure. Consequently, applying resistive loading to broaden the cone blade's transfer function is unnecessary, which means that reflectionless transmission and reception are achieved with no loss in efficiency. The dynamic transient input resistance of the antenna is shown in Fig. 10.

Kanda has shown that the transmitting transient response is proportional to the time derivative of the receiving response [4]. In order to illustrate this property of the antenna, the radiated field of the transmitting antenna is compared to the derivative of the induced current on the receiving antenna (Fig. 11). By analyzing Fig. 11, one can conclude that this property of antennas stated by Kanda is applicable to any antenna, irrespective of the structure of the antenna.

4. CONCLUSION

This paper has presented two very broad band antennas which has been use. In particular, the transmitting and receiving properties of each antenna are discussed. Although many antenna structures exhibit resonating properties when used in the ultrawideband range, in many cases, proper design and modification of such antennas can minimize the reflections due to structural discontinuities, whereby the antenna can be converted to a guiding-wave structure. These UWB antennas studied in this paper have an excellent wideband response with little or no time (phase) dispersion, while others exhibit resonating properties which are not suitable for UWB applications. This paper also verifies that the impulse response of an antenna structure in the transmit mode is proportional to the time derivative of the impulse response of the same antenna when it is operating in the receive mode, irrespective of the antenna type. Moreover, observations of the output wave shapes (far field and received current) from the antennas provide important information about their transmitting and receiving properties, and certain relationships are obtained between the input and output wave shapes.

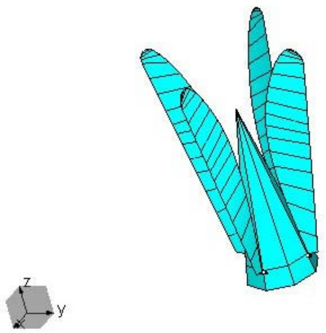

Figure 7. A cone-blade antenna structure.

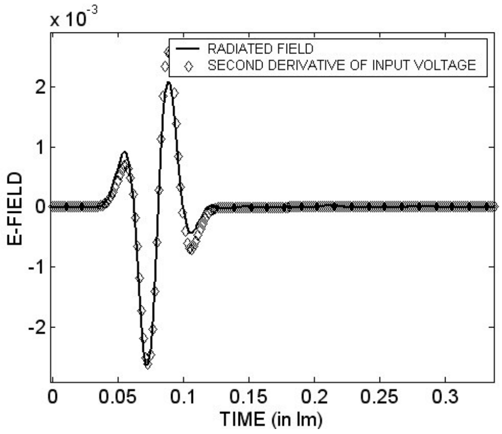

Figure 8. Radiation from a cone-blade antenna.

REFERENCES

[1] James R. Andrews, *UWB Signal Sources*, *Antennas and Propagation*, Picosecond Pulse Lab, Application Note AN-14a, August 2003, Boulder, Colorado. (Also presented at the 2003 Honolulu IEEE Wireless conference). http://www.picosecond.com/objects/AN-14a.pdf/.

[2] P. VanEtten and M. C. Wicks, "Bi-blade century bandwidth antenna," US Statuary Invention Registration H1,913, Nov. 7, 2000.

[3] M. C. Wicks and P. VanEtten, "Orthogonally polarized quadraphase electromagnetic radiator," US Patent 5,068,671, Nov. 26, 1991.

[4] M. Kanda, "Time domain sensors and radiators", in *Time Domain Measurements in Electromagnetics*, edited by E. K. Miller, Ch. 5. New York: Van Nostrand Reinhold, 1986.

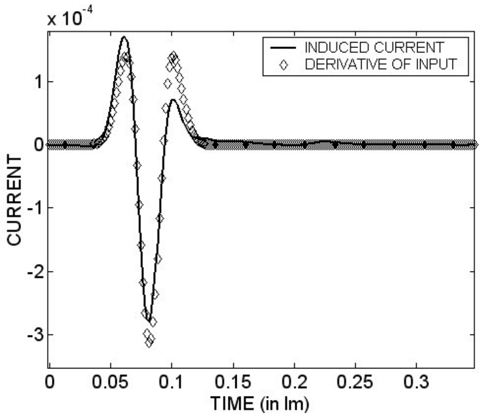

Figure 9. Reception of a monocycle by a cone-blade antenna.

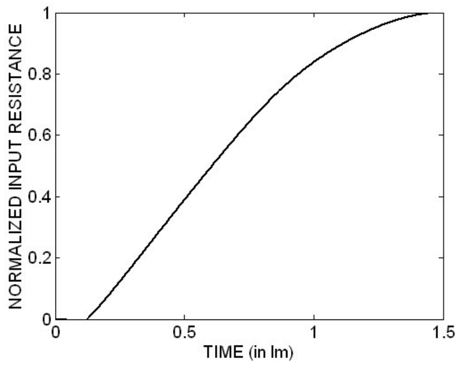

Figure 10. Transient input resistance of a cone-blade antenna.

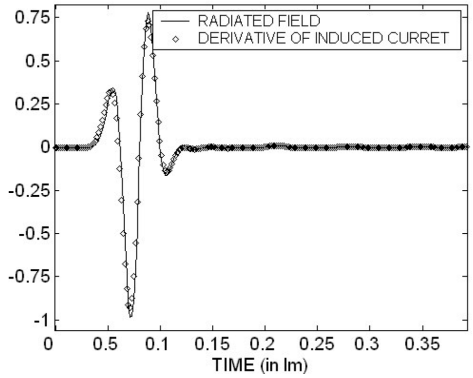

Figure 11. Comparison of the radiated field and the first derivative of the induced current when operating as a receiver.